Chem Sci Trans., 2013, **2(3),** 900-910
DOI:10.7598/cst2013.439

Chemical Science Transactions
ISSN/E-ISSN: 2278-3458/2278-3318

RESEARCH ARTICLE

Removal Methyl Orange from Aqueous Solutions Using Dragon Fruit (*Hylocereusundatus*) Foliage

ZAHRA HADDADIAN[a], MOHAMMAD AMIN SHAVANDI[a], ZURINA ZAINAL ABIDIN[a,b*], AHMADUN FAKHRU'L-RAZI[a,b] and MOHD HALIM SHAH ISMAIL[a]

[a]Department of Chemical and Environmental Engineering, Faculty of Engineering,
[b]Institute of Advanced Technology, University Putra Malaysia, 43400, Serdang, Selangor, Malaysia
zurina@eng.upm.edu.my

Received 12 November 2012 / Accepted 15 December 2012

Abstract: In this study, dragon fruit foliage was used as an adsorbent for the removal of methyl orange from an aqueous solution. The influence of the initial dye concentration, contact time, pH, temperature, dosage of biosorbent and ion strength were investigated in batch experiments. The adsorption was evaluated using Freundlich and Langmuir isotherm models and found to fit the Freundlich model. The kinetic study data were well-represented by the pseudo-second-order kinetic model. Different thermodynamic values were calculated and the adsorption process was found to be favourable and endothermic. The adsorbent was characterised using Fourier transform infrared spectroscopy and scanning electron microscopy. Results suggest the potential of dragon fruit foliage as an alternative low cost and environmental friendly biosorbent for removal of methyl orange.

Keywords: Adsorption, Methyl orange, Dragon fruit foliage, Kinetics, Equilibrium, Thermodynamics

Introduction

Many industries use synthetic dyes and pigments that may find their way into natural waterways[1]. The paper, printing, pharmaceutical, textile and food industries are among major users of dyes in their daily activities. Most of the dyes are synthetic in nature and have complex aromatic structures which makes them virtually non-biodegradable and non-oxidisable[2]. This escalates the concern on the impacts that these dyes have on the environment. The characteristics of these dye compounds have generated some challenging environmental problems, such as increasing the chemical oxygen demand of wastewater, thus reducing the percentage of light penetrating into the water which reduces photosynthesis activity in aquatic media[3-4]. This can make the waste water toxic and even mutagenic if degraded by anaerobic digestion. Furthermore, based on regulations for waste colour, a low concentration of visible dye is intolerable and can cause a health hazard for humans. Methyl orange is an anionic molecule. When there is a nitrogen compound in its structure, it becomes an azo-dye that can cause allergies and hypersensitivity[5]. These azo-

dyes are very stable and show low biodegradability which makes their removal from wastewater difficult and costly. A wide range of chemical/physical and biological treatment methods, such as membrane filtration, chemical oxidation, flocculation, ozonation, ion-exchange, irradiation and adsorption have been conventionally applied by researchers for the removal of colour from aqueous solutions[6-9]. Adsorption method is commonly used due to the biocompatibility, biodegradability and efficiency of these processes for the removal of azo-dyes from aqueous solutions.

Agricultural wastes are known to be an excellent source of lignin and cellulose; both structures consist of polar functional groups such as alcohols, aldehydes, ketones and phenolic hydroxides which are responsible for chemical adsorption. In recent years, many low-cost agricultural wastes such as banana pith[10], rice husk[11], peanut husk[12] and durian peel[13] have been investigated as biosorbents. Dragon fruit foliage (DFF) is another agricultural by-product obtained by pruning dragon fruit trees and is mostly treated as waste. In the present work, we investigated the efficiency of dragon fruit foliage as a low-cost, readily available biosorbent material for the removal of methyl orange from aqueous solutions.

Experimental

Mature dragon fruit foliage used in this study was collected from the Malaysian Agricultural Research and Development Institute (MARDI) in Serdang, Malaysia. The leaves were washed several times with distilled water to remove any unwanted materials before cutting and drying in an oven at 323 K for 24 hours. Dried leaf segments were then crushed and sieved through a Number 6 mesh (ASTM E11:01). The biosorbent material was then kept dry in a glass-capped container.

The surface properties of the biosorbent samples were analysed by scanning electron microscopy (SEM) (Hitachi, Model S-3400N) using an acceleration voltage of 7 kV and magnification ranging from 100 x to 2000 x. Fourier transform infrared (FTIR) spectroscopy analysis using a Perkin-Elmer Spectrum 100 was carried out on the biosorbent to identify the surface functional groups in the wavelength range of 4000-650 cm^{-1} that might be involved in MO adsorption.

Preparation of the adsorbate solution

The dye, methyl orange (MO) (C.I.13025, MF: $C_{14}H_{14}N_3NaO_3S$, 327.34 g mol^{-1}, λ maximum 464 nm) was obtained from Fluka chemicals. In order to prepare a dye stock solution of 1000 ppm, 1.0 g of MO was accurately weighed and dissolved in 1000 mL of double distilled water and the desired experimental concentrations were obtained by further dilution. The pH of the solutions was adjusted using 0.1 N sodium hydroxide and hydrochloric acid and measured by a EUTECH 510 pH meter.

Determination of point of zero charge

The pH of zero point charge (pHpzc) of dragon fruit foliage (DFF) was determined by the potentiometric mass titration (PMT) technique[14]. The point of zero charge (pH_{pzc}) is the pH at which the surface has no electrical charge; hence no activation of acidic or basic functional groups is detected. Here, 240 mL 0.01 N KNO_3 was added to 250 mL capped bottles and the range of initial pH values of KNO_3 were adjusted between 2 to 10 by using 0.5 N KOH and HNO_3. The final volume of the KNO_3 solution was made up to 250 mL by further adding 0.01 N KNO_3. Next, 1.0 g of accurately weighed crushed biosorbent was added to each of the bottles. The suspensions were left in a shaker and allowed to equilibrate

at room temperature for 33 hours. The pH values of the solutions were recorded and analysed by plotting ΔpH *versus* pH_0. The pH value where the plot crossed the ΔpH line at zero was the pH_{zpc}.

Adsorption experiments

Biosorption studies were carried out in triplicate in batch mode in order to identify the effect of process parameters such as the biosorbent dosage (0.1 - 1.6 g), pH (5-10), initial dye concentration (25 - 250 ppm), temperature (298 - 328 K) and contact time (10 - 700 min) on the biosorption of MO. For these experiments, 1.0 g of biosorbent was added to 250 mL capped glass bottles containing 50 ppm of dye solutions. The bottles were shaken in a rotary shaker at a constant speed of 120 rpm. Once the equilibrium was reached, the biosorbent was separated from the samples by filtration using glass fiber filters Whatman GF/A. Then, the final dye residue concentration was measured using a UV/vis spectrophotometer (Thermo Electron Corporation). All assays were carried out in triplicate and the presented data represented the mean values of the experimental results. The amount of dye biosorbed by the DFF (mg dye per g biosorbent) and the percentage of dye removal were calculated by using following equations, respectively:

$$q_t = \frac{(C_o - C_t)V}{m} \quad (1)$$

$$\% \text{ Removal} = \frac{C_o - C_e}{C_o} \times 100 \quad (2)$$

Where q_t is the amount of dye adsorbed by the DFF (mg g^{-1}), C_0 (mg L^{-1}) and C_t (mg L^{-1}) are the initial and equilibrium concentrations of the dye in solution, respectively, V (L) is the solution volume and m (g) is the biosorbent mass.

Biosorption kinetic and equilibrium studies were performed by adding 1.4 g of DFF to 250 mL bottles containing different initial dye concentrations. The suspension was later shaken at 120 rpm at room temperature (298 K). The samples were analysed for the remaining dye concentration at various time intervals (every 10 minutes for the first hour, then intervals of 200 minutes for the remaining period).

Results and Discussion

Characterisation of adsorbents

Scanning electron microscopy (SEM) is a valuable tool for the precise measurement and analysis of very small features and the morphology of the sample. Figure 1 shows scanning electron microscopy images of DFF before and after dye adsorption.

As shown, DFF has a porous surface (Figure 1a) before contacting with dye solution. When exposed to the colour solution, the dye molecules diffused through DFF porous structure and occupied the DFF surface (Figure 1b). It is important to note that direct verification of the presence of dye molecules on the sorbent surface is not possible by SEM, since the dimensions of dyes are in nanometre scale while micrograph scale is micrometers.

Fourier Transform Infrared Spectrometry (FTIR) is another powerful tool for identifying types of functional groups of biosorbent that are responsible for entrapping the molecules of dye. Figure 2 depicts the Fourier transform spectra of DFF before and after the biosorption of dye molecules. The spectra of DFF show a number of peaks, indicating the complex nature of DFF. As shown for the unloaded adsorbent, the peaks at 855 to 890, 1260 to 1430, 1840 to 1920 and 2920 to 3120 cm^{-1} were due to C-H stretching which could be

attributed to the presence of -CH and CH groups in the lignin structure of DFF. Absorption bands appearing around 1151 and 1048 cm^{-1} could be due to C-O stretching and C-N or sulphonic groups[15]. The broad and intense band ranging from 3525 to 3620 cm^{-1} can be ascribed to the hydrogen-bonded -OH vibration of the cellulosic structure of DFF, which after adsorption decreased to 3280 to 3660 cm^{-1}. The bands ranging from 1700-1740 cm^{-1} could be attributed to C=O stretching vibrations. The peaks denoting C=O and -OH indicate the presence of carboxyl groups on the adsorbent surface.

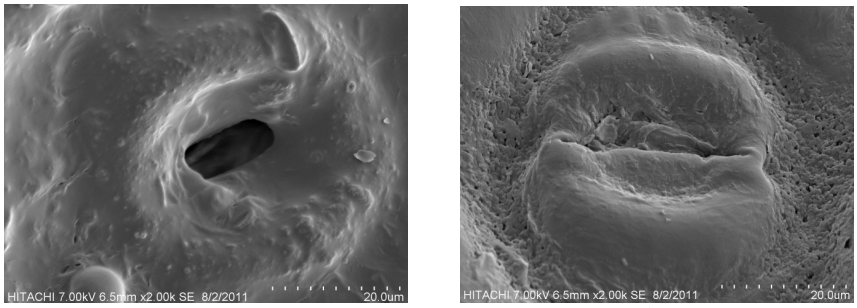

a) b)

Figure 1. SEM of DFF a) before contact with dye solution b) after contact with dye solution

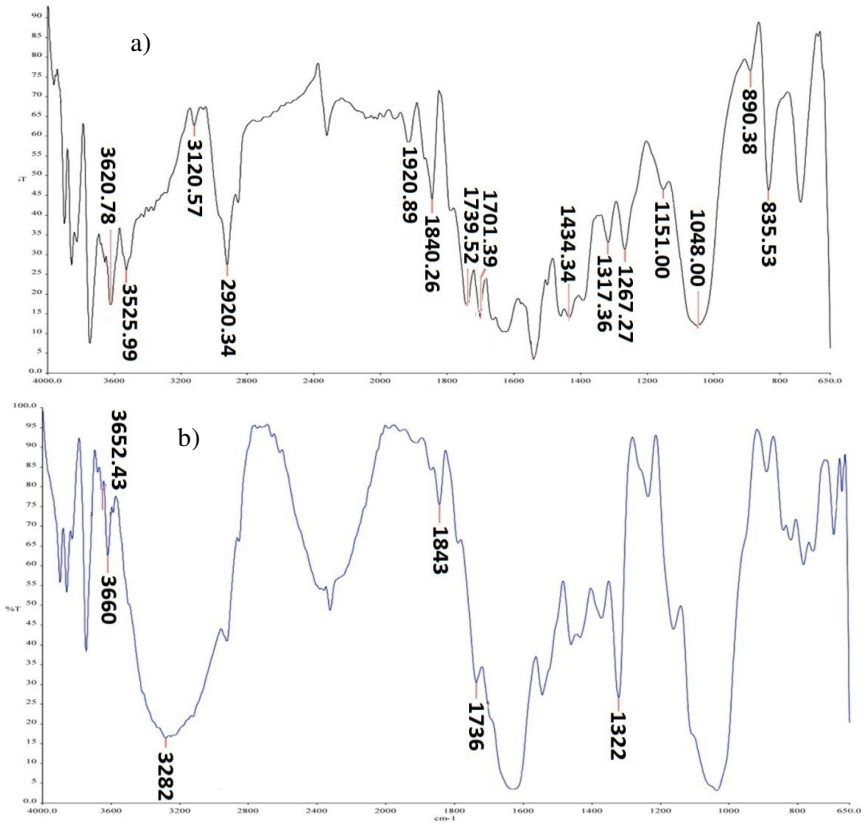

Figure 2. FTIR spectra of DFF a) before adsorption process and b) after adsorption

After adsorption, some changes were observed in the spectra as a result of the interaction between the dye and the adsorbent. The band at 1322.07 cm^{-1} indicates C-N stretching that appeared at lower frequencies in comparison to the position before the sorption process at 1623.21 cm^{-1}. Another band at 3282.82 cm^{-1} indicates N-H (amide) bending, and the bend range attributed to C=O shifted to 1736.33-1843.56 cm^{-1}.

Effect of pH

pH has a very significant effect on the adsorption process since the pH of the solution influences the surface charge of the adsorbent. Consequently, the effect of the pH of the solution on the biosorption of MO by DFF was studied in the pH range of 5-10. The biosorption percentage of DFF was found to increase with increasing solution pH up to pH 6 (Figure 3). This is due to the pH_{zpc} of DFF and anionic nature of MO. The adsorbent pH_{pzc} is 7.4, which means that the surface of DFF particles has a negative charge at pH above 7.4. If the solution pH is higher than pH_{pzc}, higher density of negative ions will occupy the adsorption sites and consequently decrease the dye adsorption. This is confirmed by the low MO adsorption at pH 10. On the other hand when the solution pH is lower than 7.4, the positive charge on adsorbent surface enhance the sorption of MO. It can be concluded that the optimum pH for MO biosorption is 6.0 and this pH was used for the rest of the study.

Effect of the initial dye concentration and contact time

The influence of the initial concentration of MO on the dye removal capacity of DFF was carried out at a fixed biosorbent dosage (1.4 g), a pH of 6, various dye concentrations (25 - 250 ppm) and different time intervals (every 10 minutes for the first hour, then intervals of 200 minutes up to 700 minutes). As is apparent in Figure 4, increasing the concentration of the dye from 12.5 to 250 ppm, increases the biosorption capacity from 2.984 to 21.051 mg g^{-1}. This could be attributed to a high mass transfer driving force generated by the initial dye concentration that overcomes the mass transfer resistance of all the molecules between the aqueous solution and solid phases[16]. MO exhibited a fast biosorption rate during the first 60 minutes of contact time due to a great availability of surface area/binding sites for dye molecules to be biosorbed. Generally, MO anions will bind to all the active sites until they are fully occupied. Hence with time, fewer active sites are available and thus reduce the amount of dye being adsorbed.

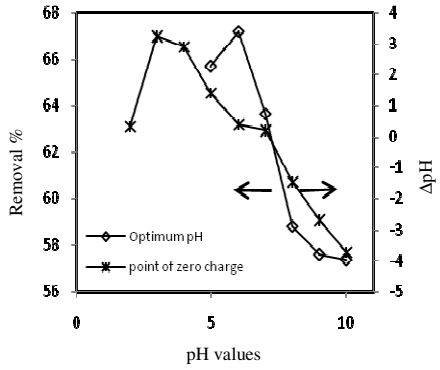

Figure 3. Effect of pH on MO adsorption and Point of zero charge (pH_{pzc}) of DFF

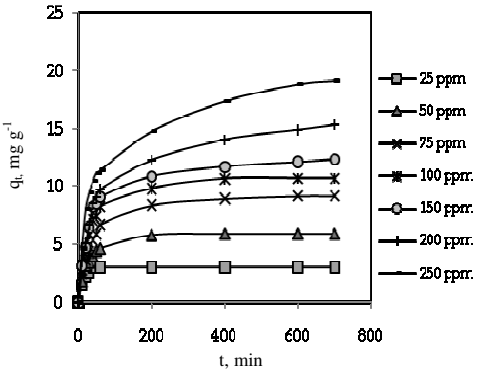

Figure 4. Effect of contact time on the equilibrium biosorption capacity of DFF at various MO concentrations at 298 K

Effect of adsorbent dosage

The study of removal of MO by DFF from aqueous solutions was performed using the biosorbent in the range 0.1-1.6 g using a dye solution concentration of 50 ppm, a pH of 6 and 200 min of contact time (the equilibrium time achieved for 50ppm of dye concentration). The results are summarised in Figure 5 in terms of % adsorption removal against different dosage of biosorbent (g). As can be seen, the dye removal percentage increased with the increase in biosorbent dosage. The highest percentage of MO removal of 80% was obtained when using 1.4 g of DFF at pH 6 within 60 minutes. The positive correlation between DFF dosage and dye removal percentage could be attributed to the increase in adsorption sites as well as an increase in the surface area of the biosorbent[33-36]. However, further increment in the dosage did not give any significant changes in the percentage removal and this could be due to the saturation of the binding sites[17].

Effect of temperature

The MO biosorption experiments were performed at different temperatures (298 K-328 K) at various concentrations of dye (25 - 250 ppm). Figure 6 shows that the adsorption capacity of the dye increased with increasing temperature. This behaviour may be due to the higher mobility of the molecules at higher temperatures and a greater availability of molecules with enough energy to interact with the active sites on the surface. In addition, increasing the temperature resulted in the swelling of the internal structure of the DFF which helps to facilitate the movement of large dye molecules[18].

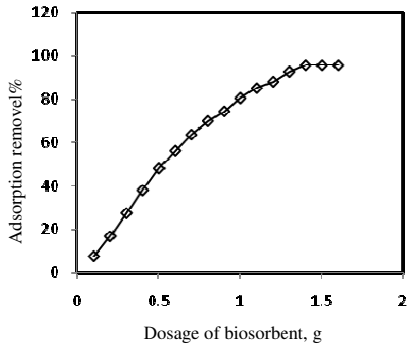

Figure 5. Effect of biosorbent dosage on the removal percentage of MO

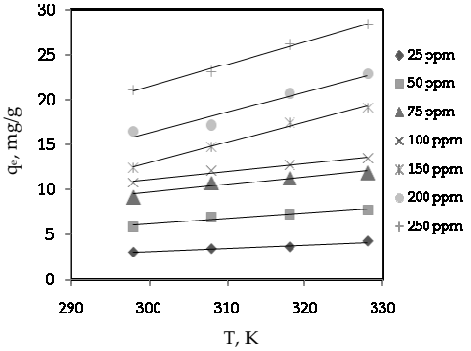

Figure 6. Effect of temperature on biosorption capacity of DFF

Effect of ion strength

The effect of ion strength on the biosorption rate of MO by DFF was investigated by the addition of different amounts of sodium chloride to the initial dye solutions. The NaCl concentration ranged from 0.1 to 0.5 N. Figure 7 shows that as the ionic strength of the solution increased, the adsorption of the dye decreased sharply. This could be due to competition between the MO anions and Cl^- for the active sorption sites[19].

Biosorption kinetics

Kinetic studies of adsorption are related to the adsorption mechanism and are necessary for optimising the adsorption process[16]. Subsequently, three of the most common kinetic models, pseudo-first-order, pseudo-second-order[11] and the intra-particle diffusion model were employed for evaluating the kinetic data. The linear form of the pseudo-first (Equation 3) and pseudo-second-order (Equation 4) models are as follows:

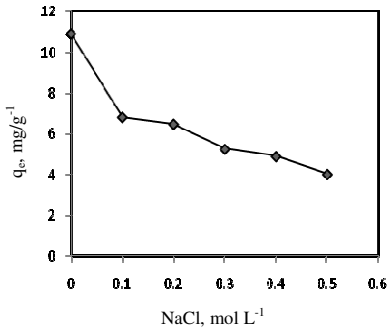

Figure 7. Effect of ion strength on biosorption capacity of DFF

$$\log(q_e - q_t) = \log q_e - \frac{k_1 t}{2.303} \quad (3)$$

and

$$\frac{t}{q_t} = \frac{1}{k_2 q_e^2} + \frac{t}{q_e} \quad (4)$$

Where q_e and q_t are the biosorption capacity at equilibrium and at time t, while k_1 (min^{-1}) and k_2 (g mg^{-1} min^{-1}) are the rate constants of the biosorption process of the pseudo-first-order and the second-order respectively.

For the pseudo-first-order model, the values of q_e and k_1 were obtained from the intercept and slope of the plot of log (q_e-q_t) *versus* t. However, in this work, the pseudo-first order model did not fit the experimental data well and thus eliminated from further discussion. For the pseudo-second-order model, q_e was calculated from the intercept and slope of the plot of t/q_t *versus* t, which is shown in Figure 8a.

Furthermore, the biosorption process can also be expressed by the momentum of the dye molecules from the aqueous solution to the surface of the biosorbent, which takes place in several stages, commencing with diffusion of the dye onto the biosorbent surface, intra-particle diffusion and the sorption of solution into the interior part and the smaller pores of the biosorbent and finally sorption of molecules into the capillaries followed by the establishment of equilibrium[11]. The intra-particle diffusion kinetic equation can be written as follows:

$$q_t = k_i t^{1/2} + I \quad (5)$$

Where k_i (mg g^{-1} min$^{-1/2}$) is the intra-particle diffusion rate constant and I is the intercept, related to the thickness of the boundary layer. The values of I and k_i are obtained from the intercept and slope of the plot of q_t *versus* $t^{1/2}$ (Figure 8b).

The fitted experimental results for the pseudo-second-order and intra-particle diffusion models are presented in Table 1. The correlation coefficients (R^2) for the pseudo-second-order model were higher than the R^2 of the pseudo-first-order model and the calculated q_e values were in good agreement with the data from the experiments. The deviation of the proposed models to the experimental data was further assessed using statistical measure of standard square error (SSE). For all the experiments, SSE values of pseudo-second-order were lower than other tested kinetic models (Table 1). These results indicated that the rate of MO adsorption on DFF is of the pseudo-second-order; implying that the adsorption of MO onto DFF is influenced by both the dye and the adsorbent concentrations[20] through chemisorption and also physisorption process.

Table 1. Kinetic parameters of MO adsorption by pseudo-second-order and intraparticle diffusion models at 298 K

		Pseudo-second-order kinetic model				Intraparticle diffusion model			
Adsorbate	C_0, mg/L	K_2 g/mg min $\times 10^{-3}$	q_e, mg/g	R^2	SSE %	K, mg/g min 0.5	I, mg/g	R^2	SSE %
MO	25	14.3	1.938	0.990	4.303	0.038	3.171	0.709	10.102
	50	10	5.952	0.999	5.121	0.067	3.505	0.663	7.859

Furthermore, according to the table, the values of K_2 decrease significantly by increasing the dye concentration. This trend suggesting that the mass transfer was the rate limiting step of the adsorption and the rate of dye mass transfer to DFF is enhanced by increasing the dye concentration[15]. Similar phenomena have been observed for the sorption of MO on activated carbon derived from *Phragmites australis* and multiwalled carbon nanotubes[2,21].

The intra-particle diffusion model was also analysed using equation 5. If the sorption process followed the intra-particle diffusion only, the plot of q_t *versus* $t^{1/2}$ would be a straight line that passes through the origin. The plots of intra-particle diffusion of MO onto DFF at different initial dye concentrations are represented in Figure 8b. Referring to the figure, the plot is not straight lines and did not pass through the origin. Furthermore, two distinct regions can be seen in the figure which indicate that the process of adsorption is not only under intra-particle diffusion but under the control of different mechanism at various contact time intervals[22].

The first shown region in Figure 8b, illustrated that the adsorption of MO is likely to be limited by boundary layer diffusion[22]. The second region indicates that intra-particle diffusion is the adsorption limiting step. At higher MO concentration, the intra-particle diffusion is dominant compared to boundary layer diffusion and thus becomes the rate limiting step during the adsorption period.

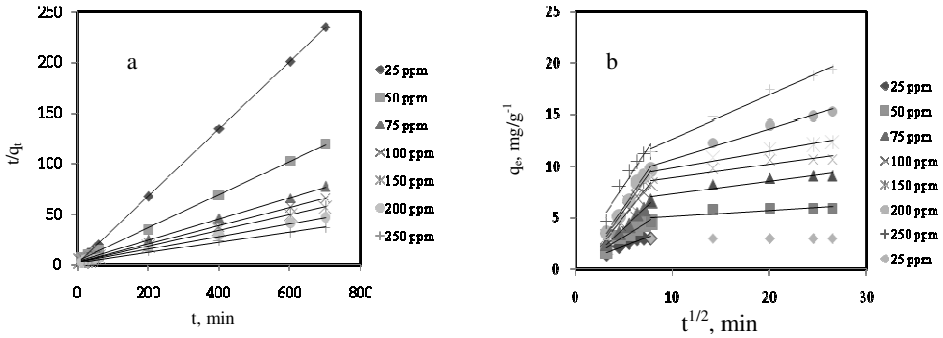

Figure 8. Kinetic of MO adsorption at different initial concentrations using a) pseudo-second-order model and b) intra-particle diffusion model at 298 K

Biosorption equilibrium

Isotherms represent the interaction between the sorbate and biosorbent. Subsequently, two of the most common adsorption isotherms, Langmuir and Freundlich were employed in this study.

The Langmuir model assumes that a defined number of sites are on a surface and as a site is occupied by the sorbate, no more sorption can occur at that site[23]. The linear form of the Langmuir isotherm can be written as the following equation:

$$\frac{C_e}{q_e} = \frac{1}{q_m k_L} + \frac{C_e}{q_m} \tag{6}$$

Where C_e is the equilibrium of dye concentration in the dye solution (mg L^{-1}), k_L is the Langmuir constant (L g^{-1}), while q_e (mg g^{-1}) and q_m (mg g^{-1}) represent the capacity of the monolayer sorption and the amount of dye biosorbed onto the biosorbent at equilibrium, respectively. The plot of C_e/q_e *versus* C_e was used to calculate the $1/k_L q_m$ intercept value and the slope of $1/q_m$.

The Freundlich model is an empirical equation which assumes a heterogeneous system and multilayer sorption. With an increasing extent of adsorption, the heat of adsorption in many instances decreases in magnitude. This reduction in heat of adsorption is logarithmic, implying that adsorption sites are distributed exponentially with respect to adsorption energy[24]. The linear form of the Freundlich isotherm can be written as the following equation:

$$\log q_e = \log k_F + \frac{1}{n} \log C_e \tag{7}$$

Where k_F (mg g^{-1}) and n are the constants of the Freundlich model which represent the capacity and intensity of sorption, respectively. The n values indicate the favourability of the adsorption process. The intercept and slope of the plot of log q_e *versus* log C_e (Figure 9) were used to calculate the values of ln k_F and $1/n$, respectively.

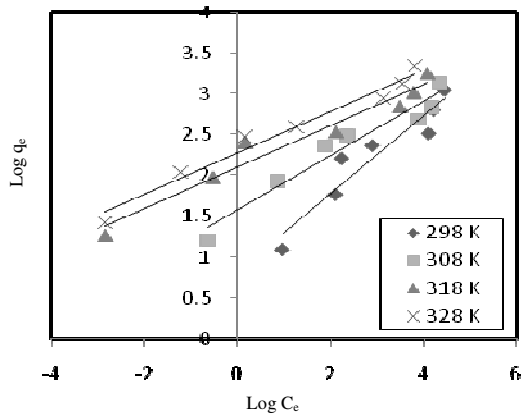

Figure 9. Freundlich Adsorption isotherms of MO onto DFF at different tempratures

The values obtained for the Langmuir and Freundlich constants are summarised in Table 2. As shown, the R^2 for the Freundlich model was higher for all the temperatures evaluated, and thus this model fitted better to experimental data. The excellent fit of the Freundlich isotherm to the experimental data confirmed that the adsorption is multilayer, with a non-uniform distribution of heat of adsorption over the surface implying that the adsorption sites are distributed exponentially with respect to adsorption energy. Furthermore, values of 1/n were between zero and one, which indicates that DFF is favourable for the adsorption of MO dye under the experimental conditions employed.

Table 2. Isotherm parameters by Langmuir and Freundlich models for different temperature

T, K	Langmuir isotherm model			Freundlich isotherm model		
	k_L, L g^{-1}	q_{max}, mg g^{-1}	R^2	k_F, mg g^{-1}	1/*n*	R^2
298	1.108	17.665	0.872	2.284	0.478	0.903
308	3.115	19.104	0.931	4.859	0.334	0.944
318	6.289	22.863	0.946	8.207	0.255	0.952
328	11.111	24.988	0.959	9.757	0.255	0.972

Biosorption thermodynamics

Biosorption thermodynamic studies were conducted at various temperatures (298-328 K). Parameters such as enthalpy changes (ΔH^0: KJ mol^{-1}), entropy changes (ΔS^0: J mol^{-1} K^{-1}) and free energy changes (ΔG^0: KJ mol^{-1}) can be calculated using the temperature data achieved by the biosorption of MO onto DFF according to the following equations:

$$\Delta G^0 = -RT \ln (k_C) \quad (8)$$

$$\Delta G^0 = \Delta H^0 - T\Delta S^0 \quad (9)$$

Where *R* (8.314 J/mol K) is the universal gas constant, *T* represents the absolute temperature (Kelvin) and k_C is the equilibrium adsorption constant. The values of ΔH^0 and ΔS^0 for the dye were calculated from the slope and intercept of the plot of ΔG^0 *versus* T, respectively (Figure 10).

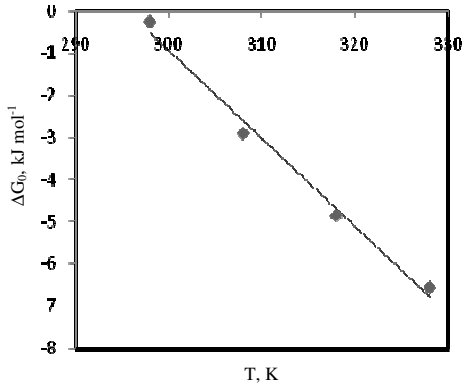

Figure 10. Plot of free energy change (Gibbs) *vs*. temperature

Table 3 shows the values of the thermodynamic parameters of MO for biosorption on DFF. The negative values of ΔG^0 at all temperatures studied indicate the spontaneity of the biosorption process. The positive values of ΔH^0 suggest that the biosorption process is endothermic. The positive values of ΔS^0 show increased randomness at the solid/liquid interface during the biosorption of the MO dye.

Table 3. Thermodynamic parameters for biosorption of MO on DFF

T, K	Thermodynamic parameters		
	ΔG^0, kJ mol^{-1}	ΔH^0, kJ mol^{-1}	ΔS^0, J mol^{-1} K^{-1}
298	-0.255	61.71	208
308	-2.91		
318	-4.946		
328	-6.566		

Conclusions

In this study, DFF was evaluated as a biosorbent for the removal of an anionic dye, methyl orange, from an aqueous solution. The biosorption experiments were performed as a function of adsorbent dosage, pH, contact time, initial dye concentration, ion strength and temperature. The percentage of removal decreased with an increase in the initial dye concentration and increased with increasing contact time and dose of the adsorbent. Furthermore, based on the results obtained with increasing temperature, the adsorption ability also increased. The kinetics of the biosorption studies were best fit using a pseudo-second-order kinetic model at different dye concentrations. The equilibrium data were well-expressed by the Freundlich isotherm model. Thermodynamic studies showed that the biosorption process was practicable and spontaneous at all temperatures studied and was also endothermic. The present study suggests that DFF is a low-cost and environmental friendly adsorbent that may be used for the removal of MO from aqueous solutions.

References

1. Koprivanac N and Kusic H, Hazardous organic pollutants in colored wastewaters, Nova Science Publishers, 2008.
2. Chen S, Zhang J, Zhang C, Yue Q, Li Y and Li C, *Desalin. ,* 2010, **252**, 149-156.
3. Waranusantigul P, Pokethitiyook P and Kruatrachue M and Upatham E S, *Environ Pollut.*, 2003, **125(3)**, 385-392.
4. Sivaraj R, Namasivayam C and Kadirvelu K, *Waste Manage.*, 2001, **21(1)**, 105-110.
5. Deligeer W, Gao Y W and Asuha Y, *Appl Sur Sci.,* 2011, **257(8),** 3524-3528.
6. Bhatnagar A and Sillanpaa M, *Chem Eng J.,* 2010, **157(2-3),** 277-296.
7. Ciardelli G, Corsi L and Marucci M, *Resour Conserv Recycl.,* 2000, **31(2)**, 189-197.
8. Daneshvar N, Ayazloo M, Khataee A R and Pourhassan M, *Bioresour Technol.*, 2007, **98(6),** 1176-1182.
9. Panswed J and Wongchaisuwan S, *Water Sci Technol.*, 1986, **18,** 139-144.
10. Namasivayam C and Kanchana N, *Chemosphere*, 1992, **25(11),** 1691-1705.
11. Shih M C, *Desalin. Water Treat.*, 2012, **37,** 200-214.
12. Hu Z ,Ju, Wang N X, Tan J, Chen J Q and Zhong W Y, *Desalin Water Treat.*, 2012, **37(1-3),** 160-168.
13. Ong S T, Tan S-Y, Khoo E C, Lee S L and Ha S T, *Desalin Water Treat.,* 2012, **45(1-3),** 161-169.
14. Fiol N and Villaescusa I, *Environ Chem Lett.*, 2009, **7(1),** 79-84.
15. Wang X S, Zhou Y, Jiang Y and Sun C, *J Hazard Mater.*, 2008, **157(2-3),** 374-385.
16. Dogan M, Alkan M, Demirbas O, Ozdemir Y and Ozmetin C, *Chem Eng J.*, 2006, **124(1-3),** 89-101
17. Mohan S and Gandhimathi R, *J Hazard Mater.*, 2009, **169(1-3),** 351-359.
18. Asfour H M, Fadali O A, Nassar M M and El Geundi M S, *J Chem Technol Biotechnol.,* 1985, **35(1),** 21-27.
19. Gonga R, Dingb Y, Lic M, Yanga C, Liua H and Suna Y, *Dye Pigm.,* 2005, **64(3),** 187-192.
20. Abramian L and El-Rassy H, *Chem Eng J.,* 2009, **150(2-3),** 403-410.
21. Yao Y, Bing H, Feifei X and Xiaofeng C, *Chem Eng J.*, 2011, **170(1),** 82-89.
22. Doğan M, Özdemir Y and Alkan M, *Dyes Pigm.*, 2007, **75(3),** 701-713.
23. Ibrahim S, Ang H -M and Wang S, *Bioresour Technol.*, 2009, **100(23),** 5744-5749.
24. Hutson N D and Yang R T, *Adsorption,* 1997, **3(3),** 189-195.